Virology 447 (2013) 112–120

Contents lists available at ScienceDirect

Virology

journal homepage: www.elsevier.com/locate/yviro

# Role of CD25$^+$ CD4$^+$ T cells in acute and persistent coronavirus infection of the central nervous system

Maria Teresa P. de Aquino [a], Shweta S. Puntambekar [a], Carine Savarin [a], Cornelia C. Bergmann [a], Timothy W. Phares [a], David R. Hinton [b], Stephen A. Stohlman [a,*]

[a] Department of Neurosciences, Lerner Research Institute, The Cleveland Clinic Foundation, 9500 Euclid Avenue, NC30, Cleveland, OH 44195, United States
[b] Department of Pathology, Keck School of Medicine, University of Southern California, Los Angeles, CA 90033, United States

ARTICLE INFO

*Article history:*
Received 15 May 2013
Returned to author for revisions
4 June 2013
Accepted 26 August 2013
Available online 24 September 2013

*Keywords:*
Regulatory T cells
Coronavirus
Acute encephalitis
Viral persistence
Demyelination

ABSTRACT

The influence of CD25$^+$CD4$^+$ regulatory T cells (Treg) on acute and chronic viral infection of the central nervous system (CNS) was examined using a glial tropic murine coronavirus. Treg in the CNS were highest during initial T cell mediated virus control, decreased and then remained relatively stable during persistence. Anti-CD25 treatment did not affect CNS recruitment of inflammatory cells. Viral control was initially delayed; however, neither the kinetics of viral control nor viral persistence were affected. By contrast, the absence of Treg during the acute phase resulted in increased demyelination during viral persistence. These data suggest that CNS inflammation, progression of viral control and viral persistence are relatively independent of CD25$^+$CD4$^+$ Treg. However, their absence during acute infection alters the ability of the host to limit tissue damage.



## Introduction

Regulatory T cells (Treg) which express the Foxp3 transcription factor, neuropilin 1 (Nrp-1) and the IL-2 receptor (CD25) comprise ~10% of CD4$^+$ T cells in the naïve animal and play an essential role in regulating the immune response to infection, progression of clinical disease and tissue damage (Langier et al., 2010; Lourenco and La Cava, 2011; Rouse et al., 2006; Rowe et al., 2012). During viral infection the host is challenged to mount an effective anti-viral immune response while minimizing immune mediated damage. Exuberant T cell effector function and tissue damage are regulated by sustained natural Treg (nTreg), induction of antigen specific Foxp3$^+$ Treg (iTreg), secretion of the anti-inflammatory cytokine IL-10 by both Foxp3$^+$ and Foxp3$^-$ T cells, as well as inhibitory ligand receptor interactions (Belkaid, 2007; Curotto de Lafaille and Lafaille, 2009; Langier et al., 2010; Rowe et al., 2012). Treg influence the immune response during a variety of acute viral infections (Rouse et al., 2006; Rowe et al., 2012; Zelinskyy et al., 2009) and are implicated in facilitating persistent infections in both humans and mice (Dittmer et al., 2004; Rowe et al., 2012; Xu et al., 2006). However, their suppressive role and the mechanism(s) of suppression vary depending upon both the pathogen and primary tissue infected. Following mucosal infection by Herpes simplex virus type 2 (HSV-2) Treg facilitate recruitment of virus effectors to the site of infection (Lund et al., 2008). They also enhance the severity of murine hepatitis virus (MHV) induced hepatitis due to their expression of the immunosuppressive cytokine fibrinogen-like protein 2 (Shalev et al., 2009). By contrast, during acute respiratory syncytial virus (RSV) infection of the lung or Herpes simplex virus type 1 (HSV-1) infection of the eye, Treg limit cellular recruitment into the site of infection, diminishing tissue destruction (Lee et al., 2010; Suvas et al., 2004). These findings suggest that Treg play an important role in regulating immunopathology associated with viral infection; however, this anti-inflammatory regulation may also reduce anti-viral activity, leading to delayed clearance and/or viral persistence.

The balance between an effective immune response, limited tissue damage, and establishment of viral persistence is especially critical in the central nervous system (CNS), due to its limited regenerative capacity. Theiler's murine encephalomyelitis virus (TMEV) infection produces an acute encephalitis in mouse strains either susceptible or resistant to chronic CNS infection. Depletion and/or functional inactivation of CD25$^+$ Treg did not affect CNS inflammation or TMEV replication in mice resistant to chronic infection (Richards et al., 2011). The identical depletion strategy resulted in both enhanced inflammation and control of TMEV replication in the CNS of mice susceptible to chronic infection (Richards et al., 2011). By contrast, Treg depletion

* Corresponding author. Fax: +1 216 444 7927.
*E-mail address:* stohlms2@ccf.org (S.A. Stohlman).

0042-6822 © 2013 The Authors. Published by Elsevier Inc. Open access under CC BY-NC-SA license.
http://dx.doi.org/10.1016/j.virol.2013.08.030

prior to acute infection with a neuronotropic MHV, which also produces chronic demyelination, did not alter CNS inflammation or virus specific T cell responses (Cervantes-Barragan et al., 2012). Following CNS infection with an MHV variant containing a mutation in the immunodominant $CD4^+$ T cell epitope which ameliorates disease, anti-CD25 mediated Treg depletion increased both morbidity and mortality (Anghelina et al., 2009). A beneficial role of Treg was also supported by adoptive transfer of nTreg at a time when CNS infection by a sub-lethal, glial tropic JHM strain of MHV (JHMV) was already established. The increased Treg ameliorated clinical disease and immunopathology without altering viral clearance (Trandem et al., 2010). Nevertheless, the role of $CD25^+$ Treg in the pathogenesis of acute JHMV encephalomyelitis and progression to persistent CNS infection is unclear. To better define the role of $CD25^+$ Treg early during JHMV induced encephalomyelitis and potential consequences on the chronic infection associated with sustained demyelination, the present study examined depletion/functional inactivation of $CD25^+$ cells in wild type (WT) and syngeneic IL-10 reporter mice. The Treg population, composed of both $Nrp1^{hi}$ and $Nrp1^{low}$ Treg, peaked in the CNS during acute infection, declined as virus was controlled, and was retained in the CNS during viral persistence. The absence of $CD25^+CD4^+$ T cells did not influence the composition or extent of the CNS inflammatory cells, including virus-specific $CD8^+$ T cells. However, CD25 depletion transiently impaired infectious virus control in the absence of detectable differences in *ex vivo* cytolytic effector function. The transient delay in virus control correlated with increased tissue damage although viral persistence within the CNS was not altered. These data support the concept that the regulation of the immune response within the CNS by $CD25^+$ T cells during JHMV infection is confined to a temporally narrow window during the initiation and effector phase of the acute inflammatory response.

## Results

### *Kinetics of $CD25^+$ Nrp-$1^{hi}$ nTreg and Nrp-$1^{low}$ iTreg accumulation in the CNS*

Prior to initiating anti-CD25 monoclonal antibody (mAb) treatment the kinetics and relative composition of $CD25^+$ and $Foxp3^+CD4^+$ T cells recruited into the CNS were assessed following JHMV infection. CNS accumulation of $CD25^+$ and $Foxp3^+CD4^+$ T cells followed similar patterns throughout infection (Fig. 1A). Total numbers of both $CD25^+CD4^+$ and $Foxp3^+$ T cells peaked at day 7 post infection (p.i.) comprising ~20% of total $CD4^+$ T cells (Fig. 1). These populations declined rapidly by day 10 p.i. and stabilized thereafter (Fig. 1B and C). Importantly, >75% of $CD25^+$ cells expressed $Foxp3^+$ at day 7 p.i. indicating a minority of ~25% non Treg $CD4^+$ effector cells expressed CD25 (Fig. 1A and D). These data show that the vast majority of the $Foxp3^+$ population expressed CD25 (Fig. 1A and D) and this proportion remained stable at 75–80% throughout the infection (Fig. 1A and D).

To distinguish a phenotypic transition of Treg populations, possibly accompanied by differential expression of CD25, nTregs were identified based on high Nrp-1 expression (Weiss et al., 2012; Yadav et al., 2012). At day 7 p.i., $Nrp\text{-}1^{hi}$ nTreg represented the majority (~75%) of $Foxp3^+$ Treg within the CNS (Fig. 2A and B). At day 10 p.i., the frequency of $Nrp\text{-}1^{hi}$ nTreg declined to ~50% and remained stable at all subsequent time points, resulting in an equal proportion of $Nrp\text{-}1^{hi}$ and $Nrp\text{-}1^{low}$ Treg (Fig. 2A and B). Similar to the total $Foxp3^+$ population (Fig. 1D), CD25 expression remained stable at ~75% on both $Nrp\text{-}1^{hi}$ (Fig. 2C) and $Nrp\text{-}1^{low}$ Treg during the course of infection (Fig. 2C and D). These data predicted that the majority of $CD25^+Foxp3^+$ Treg are susceptible to anti-CD25 treatment. Moreover, CD25 treatment at early times during infection was anticipated to primarily target prevailing $Nrp\text{-}1^{hi}$ Treg and only a minor population of $CD25^+$ effector T cells.

### *Early $CD25^+$ T cell depletion does not alter morbidity or inflammation*

The role of $CD25^+$ Treg in JHMV induced sub-lethal encephalomyelitis and viral persistence was thus examined by infection of mice treated with anti-CD25 mAb at day -3, 0, and +3 relative to infection. JHMV induces clinical symptoms associated with encephalitis which transitions to predominantly hind limb paralysis. Severity of clinical symptoms reflects both viral load and the antiviral immune response (Bergmann et al., 2006; Kapil et al., 2009; Weiss and Leibowitz, 2011). Anti-CD25 treatment did not alter disease onset, severity or the progression of clinical symptoms

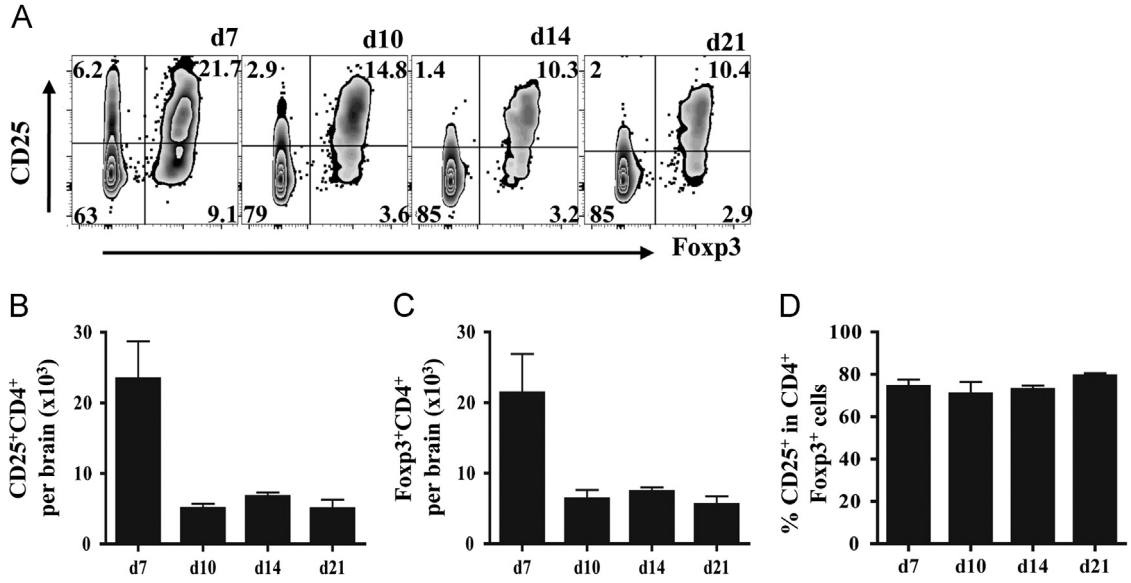


**Fig. 1.** Recruitment of $CD25^+$ Treg into the CNS. $CD25^+Foxp3^+CD4^+$ T cells in the CNS of infected mice analyzed by flow cytometry. (A) Representative density plots of Foxp3 and CD25 expression, gated on $CD4^+$ T cells. Numbers represent percentages of each population. Bar graphs depict total $CD25^+$ (B) and total $Foxp3^+$ $CD4^+$ T cells (C) recruited into the infected CNS. (D) Frequency of $CD25^+$ within $CD4^+$ $Foxp3^+$ T cells. Data represent mean ± SEM of 6–9 individual mice per time point from at least 2 separate experiments.

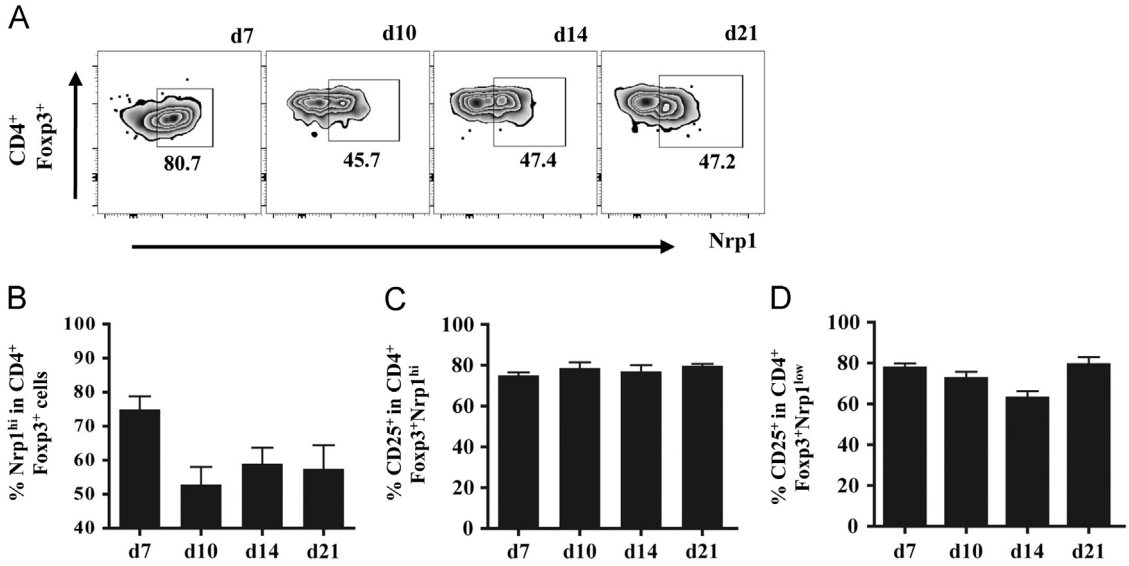


**Fig. 2.** Kinetics of Nrp-1$^{hi}$ and Nrp-1$^{low}$ CD4$^+$Foxp3$^+$ in the infected CNS. Neuropilin-1 (Nrp-1) expression on CD4$^+$Foxp3$^+$ T cells within the infected CNS analyzed by flow cytometry. (A) Representative density plots of Nrp1 expression. Gated on CNS derived CD45$^{hi}$Foxp3$^+$CD4$^+$ T cells. Numbers represent percentages of each population. Bar graphs depicting frequencies of Nrp-1$^{hi}$ cells in CD4$^+$Foxp3$^+$ T cells (B), CD25$^+$ cells in Nrp-1$^{hi}$Foxp3$^+$CD4$^+$ T cells (C) and CD25$^+$ in Nrp-1$^{low}$Foxp3$^+$CD4$^+$ T cells (D). Data represent mean $\pm$SEM of 3–6 individual mice per time point.

(Fig. 3A). These data contrast with the reduced morbidity mediated by adoptive transfer of nTreg during JHMV infection (Trandem et al., 2010). Therefore we assured the efficacy of anti-CD25 treatment. Anti-CD25 mAb eliminated essentially all CD25$^+$ T cells from the cervical lymph nodes (CLN) at least until day 14 p.i.; a small percentage of CD4$^+$CD25$^+$ T cells, representing ~15% of control levels, emerged by day 21 p.i. (data not shown). Flow cytometric analysis of CD4$^+$ T cells recruited into the CNS indicated the anti-CD25 treatment was also effective at the site of infection at least until day 14 p.i. (Fig. 3B and C). At day 21 p.i., the frequency of CD25$^+$ CD4$^+$ cells within the CNS of the anti-CD25 treated group, returned to control levels, suggesting accumulation of CD25$^+$CD4$^+$ T cells from the reemerging peripheral pool. Neither total numbers of CD45$^{hi}$ inflammatory cells nor CD11b$^+$ macrophages recruited into the CNS were altered in the anti-CD25 treated group compared to controls (Fig. 4A and B), consistent with the similarity in clinical disease. Although CD25$^+$ T cells comprise up to 30% of CD4$^+$ T cells in the CNS at day 7 p.i. (Figs. 1A and 3C), total CD4$^+$ T cells in the CNS were unaltered at all times p.i. comparing anti-CD25 treated and control groups (Fig. 4C). These data suggest the possible enrichment of CD4 effector T cells at the site of infection. These data also demonstrate efficient and sustained depletion/functional inactivation of CD25$^+$ T cells from both the periphery and CNS until day 14 p.i, spanning the time frame of maximal T cell activation and CNS accumulation (Bergmann et al., 2006; Phares et al., 2010). Moreover, their absence did not alter either a clinical component of JHMV-induced encephalitis or the cellular CNS inflammation.

### *Early CD25$^+$ T cell depletion does not alter viral control or T cell effector function*

CD25$^+$ T cell mediated regulation of anti-viral T cell activity was examined by determining viral loads in the CNS (Fig. 5A). Virus replication was not influenced by the absence of CD25$^+$ T cells at days 3 and 5 p.i., confirming the absence of defects in innate immunity critical for the early control of JHMV spread (Ireland et al., 2008). However, at day 7 p.i. when anti-viral T cell activity is maximal (Bergmann et al., 2006; Phares et al., 2010). CNS viral replication was increased in anti-CD25 compared to control mAb treated mice (Fig. 5A). A marginal, but not statistically significant, increase in infectious virus was sustained to day 10 p.i. (Fig. 5A). Nevertheless, impaired virus control was transient, as no differences were detected at day 14 p.i. and infectious virus was undetectable in the CNS of either group at day 21 p.i. (Fig. 5A). Consistent with delayed, but eventually effective viral control, no clinical evidence of viral recrudescence was found in CD25 depleted mice.

T cell mediated cytolytic activity and IFN-γ are the primary immune effectors controlling JHMV replication within the CNS (Bergmann et al., 2006) and Treg depletion enhances CD8$^+$ T cell number and activity (Dietze et al., 2011; Haeryfar et al., 2005). Comparison of anti-CD25 treated and control mice indicated no affect on CNS IFN-γ mRNA levels or frequencies of virus-specific T cells secreting IFN-γ (data not shown). The limited control of viral replication at day 7 p.i. in the absence of CD25$^+$ T cells (Fig. 5A) did not coincide with impaired CNS recruitment of total CD8$^+$ T cells (Fig. 5B). Although recruitment of CD8$^+$ T cells into the CNS was increased at days 10 and 14 p.i., these increases did not reach statistical significance. Similarly, the apparent increase in virus specific CD8$^+$ T cells at days 10 and 14 p.i. also did not reach statistical significance (Fig. 5C). During influenza virus infection of the lung, highly cytolytic IL-10 producing CD8$^+$ T cells are dependent upon CD4$^+$ T cells (Sun et al., 2011), suggesting a possible influence of CD4$^+$CD25$^+$ T cells on CD8$^+$ T cell function during JHMV. Furthermore, an IL-10$^+$CD8$^+$ T cell population constituting ~25% of virus-specific CD8$^+$ T cells resides within the JHMV infected CNS at day 7 p.i. (Puntambekar et al., 2011), comprising CD8$^+$ T cells with high cytolytic potential (Trandem et al., 2011a). Anti-CD25 treated and control IL-10 reporter mice were therefore infected to examine the possibility of diminished IL-10$^+$ effector CD8$^+$ T cells. Similar to WT mice, anti-CD25 mAb treatment was effective at eliminating CD25$^+$CD4$^+$ T cells from the CNS of infected IL-10 reporter mice until at least day 14 p.i (data not shown). Anti-CD25 treatment reduced the frequency of IL-10$^+$CD4$^+$ T cells by ~30% at day 7 p.i.; however, the population returned to WT levels by day 10 p.i (data not shown). In contrast to the CD4$^+$ T cell population, virus specific CD8$^+$IL-10$^+$ were slightly reduced at both days 7 and 10 p.i.; however, these decreases also did not reach statistical significance. CNS derived mononuclear cells from infected anti-CD25 and control mAb treated mice were also tested for direct *ex vivo* cytolytic activity

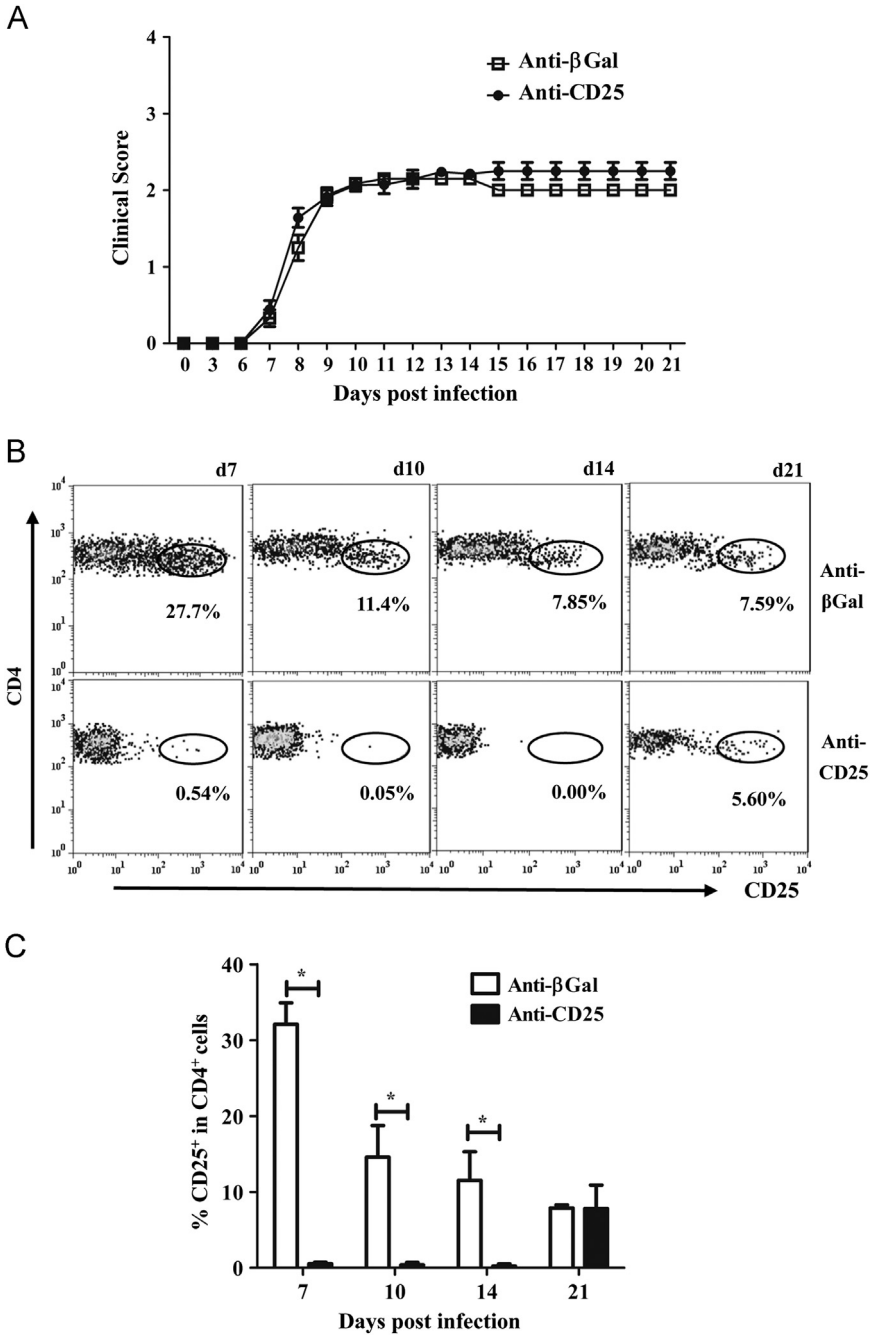


**Fig. 3.** Encephalomyelitis is independent of $CD25^+CD4^+$ T cells. WT mice received 250 μg of anti-CD25 or isotype control mAb i.p. at days −3, 0 and 3 relative to JHMV infection. (A) Clinical symptoms of anti-CD25 treated and control mice. Data are mean ± SEM and represent 3 combined experiments comprising 53 mice per group. (B) Flow cytometric analysis of CD25 expression on $CD45^{hi}CD4^+$ T cells isolated from the infected CNS. Circled populations represent percentages of $CD25^+$ T cells within $CD4^+$ T cells. Representative data from 2 separate experiments. (C) Bar graph representing the frequency of $CD25^+$ T cells within the CNS. Data are mean ± SD and represent a combination of 2–7 experiments with 3 mice per time point in each experiment.

at day 7 p.i. Although virus replication was increased at day 7 p.i. in the anti-CD25 treated group (Fig. 5A), cytolytic activity by CNS derived $CD8^+$ T cells was not altered by anti-CD25 treatment (Fig. 5E). Furthermore, cytolytic activity in both anti-CD25 and control mAb treated groups decreased at day 10 p.i. (data not shown), consistent with previous results (Bergmann et al., 1999). Thus the transiently increased viral load in the absence of $CD25^+CD4^+$ T cells could not be correlated with either reduced IFN-γ, virus-specific $CD8^+$ T cell recruitment or cytolytic activity. Transiently decreased anti-viral activity may thus be due to insufficient help provided by $CD25^+CD4^+$ T cells (Phares et al., 2012) or induction of inhibitory molecules (Phares et al., 2009), neither of which would be directly reflected by *in vitro* analysis.

### *Early $CD25^+$ T cell depletion does not alter persistence but limits demyelination*

A number of chronic viral infections are associated with $CD25^+CD4^+$ Treg (Belkaid, 2007; Rowe et al., 2012). However, no clinical or virological evidence for viral recrudescence was found in the anti-CD25 treated group (Figs. 3A and 5A), similar to control mice. Therefore, the ability of $CD25^+$ T cells to influence

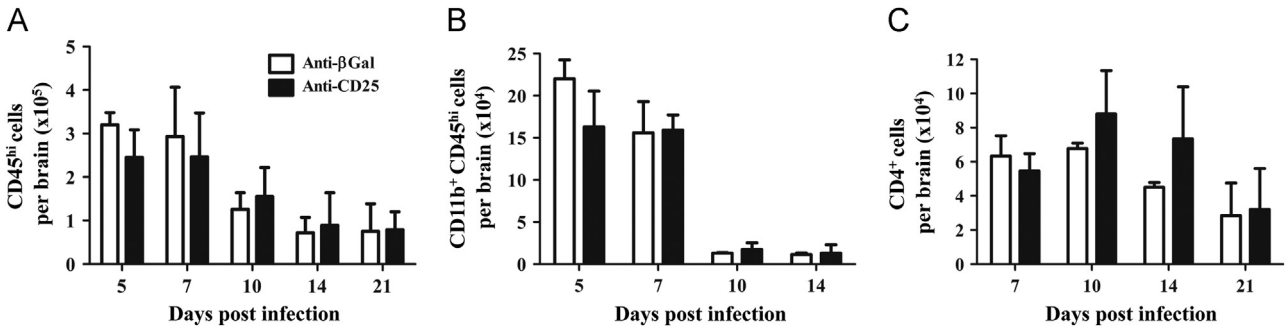


**Fig. 4.** Recruitment of CNS inflammatory cells in the absence of $CD25^+$ T cells. CNS inflammatory cells in infected anti-CD25 or control treated mice. Bar graphs depict total $CD45^{hi}$ inflammatory cells (A), $CD11b^+CD45^{hi}$ macrophages (B) and $CD4^+$ T cells (C) per brain of infected mice. Data are mean ± SD of 2–3 combined experiments with pooled brains from 3 mice per time point in each experiment.

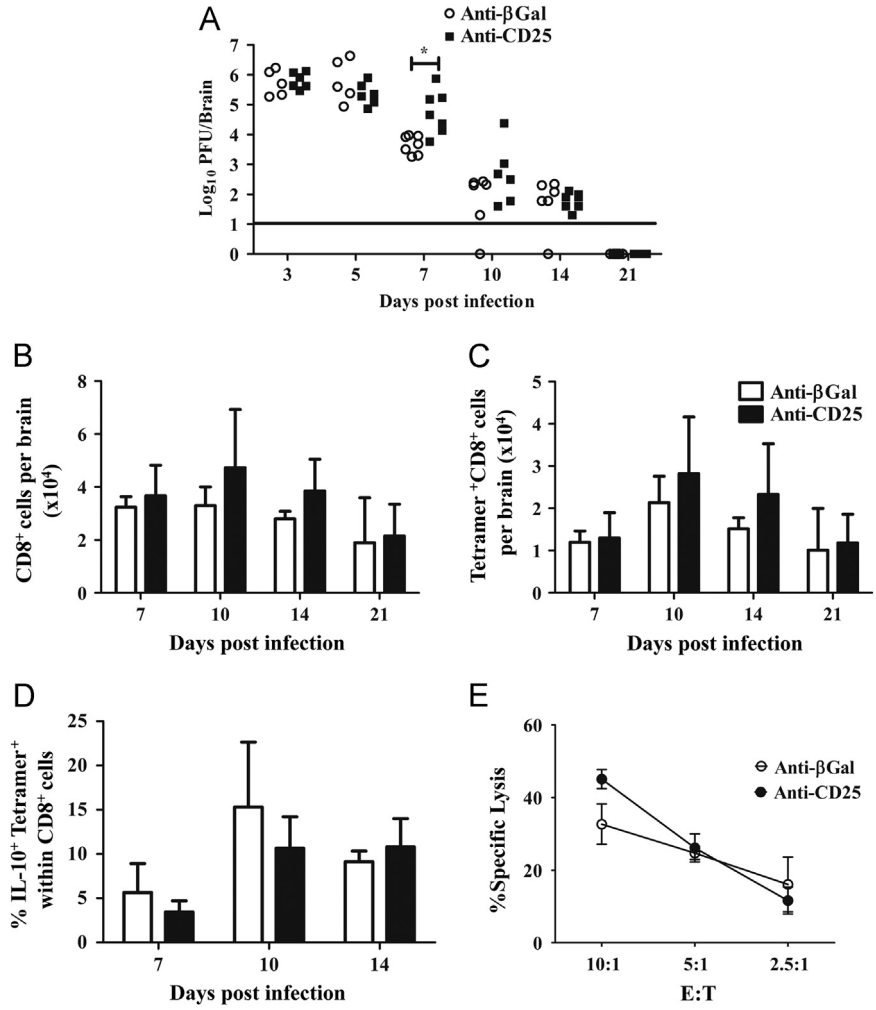


**Fig. 5.** Viral control is independent of $CD25^+CD4^+$ T cells. (A) Infectious virus within the CNS of individual anti-CD25 and control mAb treated mice. Data represent 2 combined experiments. Line represents the limit of detection. Statistical differences determined by two tailed unpaired *t* test. $^*p = < 0.05$. Bar graphs depict total $CD8^+$ T cells (B) and virus specific $CD8^+$ T cells (C) per brain. (D) Frequencies of IL-$10^+$tetramer$^+$ cells within in CNS $CD8^+$ T cells. Data are mean ± SD and represent 2–4 combined experiments with 3 mice per time point in each experiment. (E) Virus specific cytolytic activity of CNS derived mononuclear cells from mice with or without anti-CD25 treatment. Data are expressed as percentage of specific lysis (mean ± SEM) of S510 peptide coated targets at various effector: target (E:T) ratios, adjusted for the frequency of tetramer$^+CD8^+$ T cells. Data are representative of 2 separate experiments with pooled cells from 6–7 mice per group.

viral persistence was examined by PCR due to the absence of infectious virus during JHMV persistence (Bergmann et al., 2006; Phares et al., 2010). As expected based on the limited ability of anti-CD25 treated mice to control viral load at day 7 p.i., expression of the mRNA encoding the viral nucleocapsid (N) protein was increased in the brains of anti-CD25 treated mice compared to controls (data not shown). At subsequent times p.i., however, viral mRNA expression was equivalent in the spinal cords of both groups (Fig. 6A), the predominant site of JHMV persistence (Bergmann et al., 2006; Marten et al., 2000). These results indicate that diminished viral control during the acute phase of coronavirus mediated encephalomyelitis in the absence of $CD25^+CD4^+$ T cells did not facilitate viral persistence.

The transient decrease in control of CNS viral replication, decreased demyelination mediated by nTreg adoptive transfer in

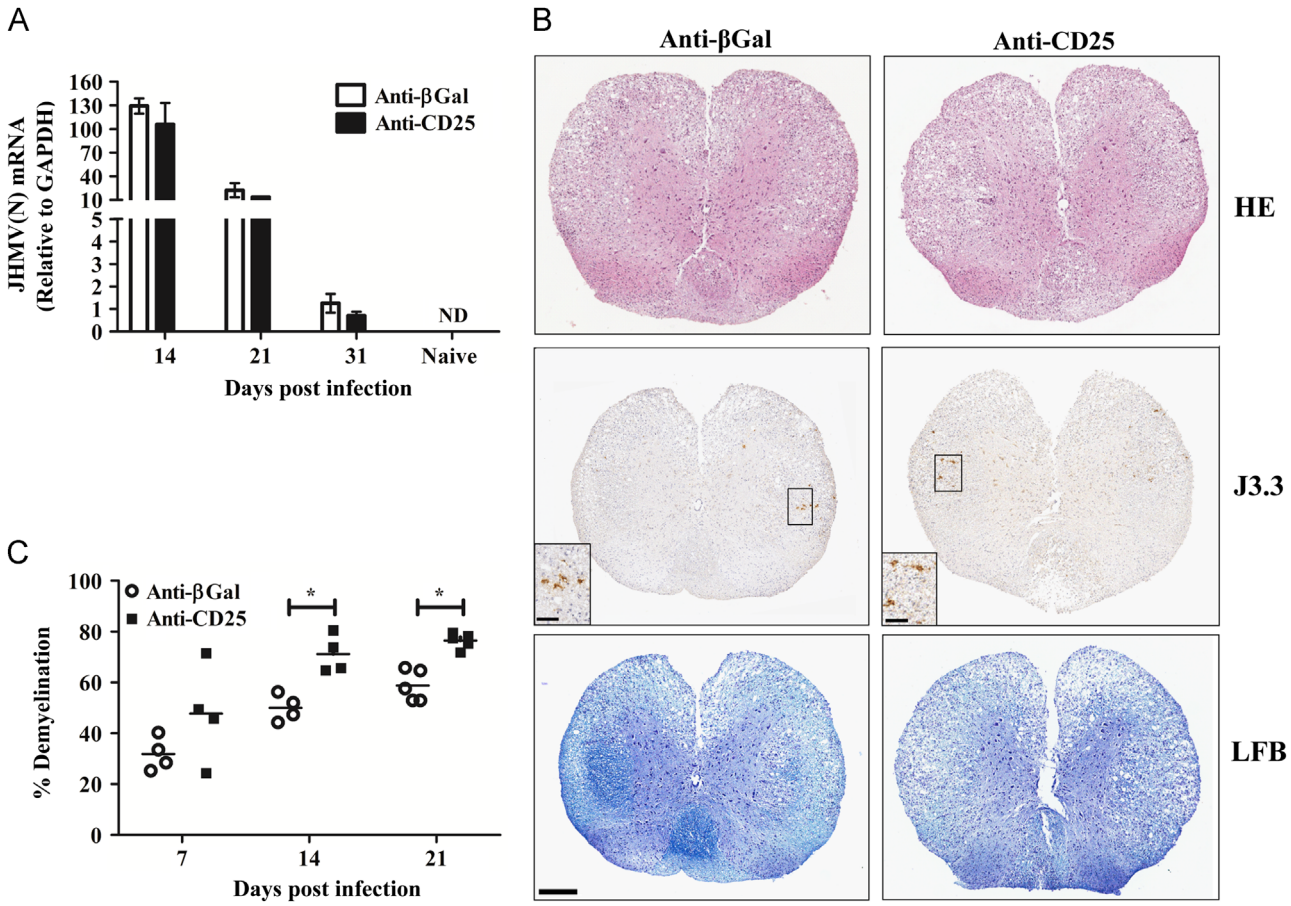


**Fig. 6.** CD25$^+$ T cell influence on JHMV persistence and pathology. (A) Relative transcript levels of viral N protein mRNA in spinal cords during persistence. Data expressed as mean ± SEM relative to GAPDH mRNA with 3 individuals per time point. Representative of 2 experiments with the same trend in each experiment. (B) Spinal cords from JHMV infected WT mice treated with either anti-CD25 or anti-βGal mAb at day 14 p.i. Inflammatory cells identified with H&E (top panel), viral infected cells identified with anti-N mAb J3.3 (middle panel) and demyelination assessed with LFB (bottom panel). Representative sections from 2 experiments with 3–5 mice per experiment. Bar = 200 μm. Insert bars = 50 μm. (C) Percentage demyelination in spinal cord white matter in individual mice calculated by analysis of transverse sections at 6 separate levels per mouse expressed as mean ± SEM with 3–5 mice per time point. Representative of 2 separate experiments with the same trends. Statistical differences determined by two tailed unpaired *t* test. *$p = < 0.05$.

a similar model of JHMV infection (Trandem et al., 2010) and the delayed onset of demyelination in anti-CD25 treated TMEV infected mice (Richards et al., 2011) suggested that CD25$^+$CD4$^+$ T cells might influence JHMV induced tissue damage. Therefore, spinal cords from anti-CD25 treated and control mice were compared for inflammation, the extent and distribution of viral antigen, as well as demyelination at day 14 p.i. when viral mRNA levels were equivalent (Fig. 6A). No differences in the extent or distribution of inflammatory cells were detected comparing the two groups (Fig. 6B). Similar inflammation is consistent with the overall recruitment of both inflammatory cells (Fig. 4A) and their composition (Figs. 4 and 5). Although few infected cells were found in either group (Fig. 6B), consistent with low levels of infectious virus (Fig. 5A), the predominant cell type infected exhibited the morphology and anatomical location of oligodendroglia and was similar in both groups (Fig. 6B). These data suggested that anti-CD25 treatment did not alter viral tropism.

To determine if the transiently increased viral load during the acute phase of infection prolonged or worsened tissue damage, demyelination was quantified in both groups at different times p.i. No difference in demyelination was apparent at day 7 p.i. (Fig. 6C). However, the extent of demyelination was increased in the spinal cords of the CD25 deficient mice at days 14 and 21 p.i (Fig. 6B and C). These data support the notion that the early events of viral induced tissue damage within the CNS are not regulated by CD25$^+$CD4$^+$ Treg cells. However, these data support the concept notion that the subsequent presence of Treg in the damaged CNS is not sufficient to stem demyelination initiated during the early phase of virus replication.

## Discussion

During viral infections Treg can suppress T cell activity at multiple levels. They can directly limit T cell priming in the draining lymph nodes and trafficking to the effector site (Lee et al., 2010; Suvas et al., 2004) where they can further dampen T cell effector function to prevent bystander damage. Indeed, recent evidence suggests that suppression is more important at the site of infection (Ding et al., 2012). However, suppressing an anti-viral response may also allow virus dissemination to cells critical for maintaining homeostasis and/or facilitate viral persistence (Belkaid, 2007; Rouse et al., 2006; Rowe et al., 2012). In this regard the CNS presents an especially challenging site to control infection due to the limited capacity for regeneration of specialized cells. JHMV induces an acute encephalomyelitis characterized by the recruitment of a variety of innate and adaptive immune effectors into the CNS (Bergmann et al., 2006), including Treg (Anghelina et al.; 2009, Puntambekar et al., 2011). Although reduced tissue damage following adoptive transfer of nTreg at the peak of acute JHMV encephalitis (Trandem et al., 2010) implicated a local protective role, protection was not associated

with either Treg recruitment into the CNS or decreased virus replication (Trandem et al., 2010). These results suggested that after infection is established the primary site of Treg function may be the CLN. Our data demonstrate that the high frequency of Treg recruited into the CNS during the peak of acute inflammation declines as virus replication is controlled. Consistent with previous data (Puntambekar et al., 2011) Treg are nevertheless retained within the CNS during persistence. Moreover, the majority of Treg expressed a Npr-$1^{hi}$ phenotype during peak CNS inflammation, consistent with their previous designation as nTreg based on expression of the helios transcription factor (Zhao et al., 2011). The Treg population within the CNS declined dramatically by day 10 p.i. as virus replication was controlled. However, the Nrp-$1^{low}$ Treg population increased to a stable ~50% of total Treg as virus replication was controlled and similar proportions of Nrp-$1^{hi}$ and Nrp-$1^{low}$ Treg were retained in the CNS.

To determine if Treg influenced acute JHMV infection and subsequently demyelination, mice were treated with anti-CD25 mAb prior to infection. This well established methodology has been used to minimize the influence of Treg on viral pathogenesis in both the CNS and at other anatomical sites. Inhibition of IL-2-IL/IL-2R interactions may explain the limited inflammation in some viral infections (Fulton et al., 2010; Ruckwardt et al., 2009), but it has no effect on inflammation in others (Betts et al., 2011). In addition, anti-CD25 treatment increases $CD8^+$ T cells responses under some, but not all circumstances (Betts et al., 2011; Dietze et al., 2011; Fulton et al., 2010; Haeryfar et al., 2005; Ruckwardt et al., 2009). Both $CD25^+CD4^+$ T cells and $CD4^+IL\text{-}10^+$ T cells are rapidly recruited into the JHMV infected CNS (Anghelina et al., 2009; Puntambekar et al., 2011). However, both virus control and inflammation are Treg independent following infection with a related MHV (Cervantes-Barragan et al., 2012). Therefore, it was not surprising that anti-CD25 treatment did not alter recruitment of inflammatory cells into the CNS. Limited Treg mediated suppression within the CNS is also consistent with an adverse environment established during CNS inflammation (Korn et al., 2007; Tang et al., 2008). Indeed, induction of IL-12 or IL-6 within the CNS during JHMV infection (Kapil et al., 2009) may contribute to limiting suppressive activity (Longhi et al., 2008; Zhao et al., 2012). Furthermore a variety of inhibitory molecules, i.e. Programmed death-1 ligand (PD-L1), as well as the anti-inflammatory cytokine IL-10 influence JHMV pathogenesis (Phares et al., 2010; Trandem et al., 2011b) potentially exhibiting more potent regional effects than Treg. For example, JHMV infection of IL-10 deficient mice demonstrated accelerated viral clearance, yet dramatically enhanced tissue destruction (Trandem et al., 2011a). During JHMV infection IL-10 secretion within the CNS is limited to the T cell compartment with $CD25^+IL\text{-}10^+CD4^+$ T cells, characteristic of nTreg, rapidly recruited into the CNS (Puntambekar et al., 2011). The absence of a suppressive effect suggested by anti-CD25 treatment may reside in the rapid replacement of this population by $CD25^-$ $IL\text{-}10^+$ $CD4^+$ T cells (Puntambekar et al., 2011), or the loss of CD25 expression. Although the precise phenotype of the $CD25^-IL\text{-}10^+CD4^+$ T cell population is unclear, it is possible it comprises virus-specific $Foxp3^+$ Treg (Zhao et al., 2012) or virus-specific $IL\text{-}10^+$ $Foxp3^-$ cells regulated by IL-27 (Wojno and Hunter, 2012). Interestingly, ~5% of Treg infiltrating the CNS during JHMV infection are virus-specific (Zhao et al., 2011). As CD25 expression was not assessed on this population, our data cannot exclude that enrichment of this population in the $CD25^-Foxp3^+$ subset may contribute to JHMV pathogenesis.

Control of CNS virus replication was partially inhibited at the peak of replication, suggesting that $CD25^+CD4^+$ T cells enhanced the initial phase of adaptive immunity. Although anti-CD25 treatment did not alter numbers of inflammatory cells recruited into the CNS or the proportions of anti-viral effectors, we cannot rule out a transient CD25 dependent $CD4^+$ helper T cell effect (Phares et al., 2012), independent of the Treg population. This is supported by increased mortality, despite similar JHMV clearance, in transgenic mice lacking both IL-27 and IL-35 (Tirotta et al., 2013) suggesting that neither of these Treg associated cytokines regulates viral clearance. One possibility to account for the limited clearance of infectious virus in the absence of $CD25^+CD4^+$ T cells is inhibition of CTL activity *in vivo* via the inhibitory ligand PD-L1 on CNS targets (Phares et al., 2009) which is not apparent in a direct *ex vivo* assay. Although PD-L1 mRNA expression was slightly increased in the CNS of the $CD25^+CD4^+$ T cell depleted mice relative to controls (data not shown), the difference did not reach statistical significance. Together, these data indicate that Treg exert minimal effects on anti-viral functions during acute JHMV induced encephalomyelitis, similar to their inability to alter TMEV induced encephalitis in resistant mice (Richards et al., 2011). Consistent with functional anti-viral effectors, treatment with anti-CD25 did not enhance or diminish viral persistence. These data contrast with data from a number of both human and viral infections suggesting that $CD25^+CD4^+$ Treg facilitate chronic viral infection (Belkaid, 2007; Rouse et al., 2006; Rowe et al., 2012). Although $CD25^+CD4^+$ T cells are rapidly recruited to the site of infection, depletion and/or functional inactivation demonstrates the effect on the inflammatory response within the CNS is transient, appearing to decrease the initial set point for control of virus replication without influencing viral persistence.

Transfer of Treg into mice with an established JHMV infection limited demyelination, consistent with the concept that demyelination is mediated by adaptive immunity (Pewe and Perlman, 2002; Savarin et al., 2008). However, infection of mice treated with anti-CD25 did not alter the extent of tissue damage during the acute phase of infection. These data indicate that in contrast to infection of the eye and mucosal sites (Lund et al., 2008; Suvas et al., 2004), Treg do not constitute a primary mechanism of damage control in the CNS during the period of maximal T cell effector function. By contrast, the extent of demyelination increased during viral persistence, even after $CD25^+$ T cells were re-established within the CNS. Thus despite the minimal influence of $CD25^+CD4^+$ Treg on JHMV viral load and persistence, these minimal alterations were sufficient to influence the extent of tissue damage. Nevertheless, less extensive tissue damage compared to that found in the total absence of IL-10 (Trandem et al., 2011a), suggests that in addition to Treg, other IL-10 secreting regulatory populations contribute to limiting demyelination following JHMV infection. Overall these results support the notion that the presence of Treg in the CNS during persistence and demyelination is linked to the control of acute viral load and the resulting viral induced tissue damage.

## Materials and methods

### *Mice and virus*

C57BL/6 mice (WT) were purchased from the National Cancer Institute (Frederick, MD). IL-10-GFP and Foxp3-GFP reporter mice on the C57BL/6 background (Madan et al., 2009; Korn et al., 2007) were bred locally under pathogen-free conditions. Female and male mice at 6 weeks of age were infected intracranially (i.c.) with 1000 PFU of the sub-lethal glial tropic mAb-selected J2.2v-1 variant of JHMV (Fleming et al., 1986). Mice were scored daily following infection for clinical signs as follows: 0, healthy; 1, hunched back; 2, partial hind limb paralysis or reduced ability to regain an upright position; 3, complete hind limb paralysis; 4, moribund or dead (Fleming et al., 1986). All procedures were

conducted in accordance with animal protocols approved by the Institutional Animal Care and Use Committee of the Cleveland Clinic Foundation. To deplete or functionally inactivate $CD25^+$ T cells mice received 3 intraperitoneal (i.p.) injections of 250 μg of anti-CD25 mAb (clone PC61, rat IgG1) obtained from BioXCell (West Lebanon, NH) on days -3, 0 and 3 relative to infection. Controls received 250 μg of an irrelevant rat IgG1 mAb (clone GL113, anti-β-galactosidase), originally obtained from Dr. R. Coffman (DNAX Corporation, Palo Alto, CA) and prepared as described (Phares et al., 2012) on days -3, 0 and 3 relative to infection.

*Tissue processing and virus titration*

Brains were homogenized in Dulbecco's PBS using ice cold Tenbroeck tissue homogenizers (Wheaton Science Products, Millville, NJ). After centrifugation at 450*g* for 7 min at 4 °C supernatants were stored at −80 °C. Cell pellets were suspended in RPMI medium containing 25 mM HEPES, pH 7.2 and used for the analysis of CNS inflammation as described below. Brain derived supernatants were used to determine virus titers by plaque assay on monolayers of the continuous Delayed Brain Tumor (DBT) astrocytoma cell line as described (Fleming et al., 1986; Kapil et al., 2009; Phares et al., 2012)

*Isolation of CNS cells*

CNS derived cell pellets resuspended in RPMI medium containing 25 mM HEPES (pH 7.2) were adjusted to 30% Percoll (Pharmacia, Piscataway, NJ). Cells were separated from myelin debris by centrifugation at 850*g* for 30 min at 4 °C onto a 70% Percoll cushion. Cells from the 30%/70% interphase were collected, washed and analyzed by flow cytometry or for cytolytic activity. Single cell suspensions from CLN were obtained as described (Bergmann et al., 1999; Kapil et al., 2009; Phares et al., 2012).

*Flow cytometric analysis*

Cells were incubated at 4 °C with 1% mouse serum and 1% rat anti-mouse CD16/CD32 mAb to prevent non-specific staining. Surface marker expression was examined using mAb purchased from BD Biosciences (San Diego, CA) unless otherwise noted. Staining used fluorescein isothiocyanate (FITC), phycoerythrin (PE), Peridinin chlorophyll protein (PerCP) and allophycocyanin (APC)–conjugated mAb specific for: CD45 (30-F11), CD4 (L3T4), CD8 (53-6.7), F4/80 (Serotec, Raleigh, NC), MHC Class II (2G9), CD25 (PC61), CD62L (Mel-14), CD44 (IM7), CD69 (H1-2F3) and Npr-1 (R&D Systems, Minneapolis, MN). Virus specific $CD8^+$ T cells were identified using $D^bS510$ MHC Class I tetramers (Bergmann et al., 1999; Beckman Coulter, Fullerton, CA). Cells from IL-10-GFP and Foxp3-GFP reporter mice were analyzed without fixation and GFP expression identified in the FL1/FITC channel as previously described (Puntambekar et al., 2011). Cells were acquired on a FACSCalibur or FACS Aria flow cytometer (BD Biosciences), and the data analyzed by FlowJo 7.6 software (Tree Star Inc., Ashland, OR).

*Cytotoxic T lymphocyte assay*

Specific lysis was determined using EL4 ($H\text{-}2^b$) targets pulsed with 1 μM of S510 peptide encoding the $H\text{-}2D^b$ restricted immunodominant epitope in serum free RPMI medium for 1 h at 37 °C. After washes, S510 coated cells were labeled with high (2.5 μM) and control cells (no peptide) with low (0.125 μM) carboxyfluorescein succinimidyl ester (CFSE; Molecular Probes, Eugene OR), respectively. High and low CSFE labeled targets ($5 \times 10^3$) were plated into 96 well plates in a volume of 100 μl. CNS derived cells were added in a volume of 100 μl at various effector: target (E:T) ratios based on the frequency of virus specific $CD8^+$ T cells identified with $D^bS510$ tetramer (Bergmann et al., 1999). After 6 h incubation at 37 °C, cells were harvested and directly acquired on a FACSCalibur flow cytometer (BD Biosciences). Data were analyzed by FlowJo 7.6 software (Tree Star Inc., Ashland, OR). Specific lysis was calculated based on the following formula: [1 − (ratio of targets only/ratio of target + T cells)] × 100.

*Gene expression*

Spinal cords were homogenized in TRIzol (Invitrogen, Carlsbad, CA) using a TissueLyzer and stainless steel beads (Qiagen, Valencia CA) and RNA isolated as previously described (Ireland et al., 2008). Briefly, following addition of chloroform samples were centrifuged at 12,000*g* for 15 min at 4 °C. RNA was precipitated with isopropyl alcohol, washed with 75% ethanol and resuspended in RNase-free water (Gibco/Invitrogen, Grand Island, NY). DNA was eliminated using a DNA-free kit (Ambion, Austin, TX) according to the manufacturer's instructions. The cDNA was obtained by reverse transcription using 2 μg of RNA, Moloney murine leukemia virus reverse transcriptase (Invitrogen, Carlsbad, CA), 10 mM of deoxynucleoside triphosphate mix, and 250 ng of random hexamer primers (Invitrogen, Carlsbad, CA) for 1 h at 37 °C. Real-time quantitative PCR (qRT-PCR) used SYBR® Green in a 7500 Fast Real-time PCR system (Applied Biosystems, Foster City, CA). Primers specific for the JHMV N gene were: (F: forward, R: reverse) 5'-CGCAGAGTATGGCGACGAT-3' (F) and 5'-GAGGTCCTAGTC-TCGGCCTGTT-3' (R). Ct values were normalized to GAPDH mRNA levels using the following formula: $2^{[Ct\ (GAPDH) - Ct\ (gene\ of\ interest)]} \times 1000$ where Ct is the threshold cycle as previously described (Puntambekar et al., 2011).

*Histopathological analysis*

Spinal cords were fixed in 10% Zinc formalin, divided into 6 sections corresponding to cervical, thoracic and lumbar regions and embedded in paraffin as described previously (Hindinger et al., 2012) Sections were stained with hematoxylin and eosin (H&E) to visualize inflammation or Luxol Fast Blue (LFB) to visualize myelin. For viral antigen, sections were incubated with anti-JHMV mAb J.3.3 specific for the viral N protein and visualized using immunoperoxidase-labeled anti-mouse mAb (Vectastain-ABC kit, Vector Laboratories, Burlingame, CA). Sections were scored in a blind manner for inflammation, demyelination, and viral antigen. Stained spinal cord sections of all 6 levels on individual slides were scanned with an Aperio ScanScope (Vista, CA) at 40× and digitally imaged at high resolution. Spinal cord sections of all 6 levels on individual slides stained with LFB were used to quantify areas of demyelination within the white matter using Aperio software (Hindinger et al., 2012). Representative fields were identified based on average score of all sections in each experimental group.

*Statistical analysis*

Statistical significance was determined using standard two-tailed Student's *t* test, assessed by GraphPad Prism 5.0 software (La Jolla, CA). The results are shown as either mean ± SEM or mean ± SD for each group. A value of $p < 0.05$ was considered statistically significant.

## Acknowledgments

We sincerely thank Wenqiang Wei, Eric Barron, Ernesto Barron, Jennifer Powers, Kate Stenson and Mi Widness for exceptional technical assistance.

## References


Anghelina, D., Zhao, J., Trandem, K., Perlman, S., 2009. Role of regulatory T cells in coronavirus-induced acute encephalitis. Virology 385, 358–367.

Belkaid, Y., 2007. Regulatory T cells and infection: a dangerous necessity. Nat. Rev. Immunol. 7, 875–888.

Bergmann, C.C., Lane, T.E., Stohlman, S.A., 2006. Coronavirus infection of the central nervous system: host-virus stand-off. Nat. Rev. Microbiol. 4, 121–132.

Bergmann, C.C., Altman, J.D., Hinton, D., Stohlman, S.A., 1999. Inverted immunodominance and impaired cytolytic function of CD8+ T cells during viral persistence in the central nervous system. J. Immunol. 163, 3379–3387.

Betts, R.J., Ho, A.W., Kemeny, D.M., 2011. Partial depletion of natural CD4+ CD25+ regulatory T cells with anti-CD25 antibody does not alter the course of acute influenza A virus infection. PLoS One 6, e27849.

Cervantes-Barragan, L., Firner, S., Bechmann, I., Waisman, A., Lahl, K., Sparwasser, T., Thiel, V., Ludewig, B., 2012. Regulatory T cells selectively preserve immune privilege of self-antigens during viral central nervous system infection. J. Immunol. 188, 3678–3685.

Curotto de Lafaille, M.A., Lafaille, J.J., 2009. Natural and adaptive foxp3+ regulatory T cells: more of the same or a division of labor? Immunity 30, 626–635.

Dietze, K.K., Zelinskyy, G., Gibbert, K., Schimmer, S., Francois, S., Myers, L., Sparwasser, T., Hasenkrug, K.J., Dittmer, U., 2011. Transient depletion of regulatory T cells in transgenic mice reactivates virus-specific CD8+ T cells and reduces chronic retroviral set points. Proc. Natl. Acad. Sci. USA 108, 2420–2425.

Ding, Y., Xu, J., Bromberg, J.S., 2012. Regulatory T cell migration during an immune response. Trends Immunol. 33, 174–180.

Dittmer, U., He, H., Messer, R.J., Schimmer, S., Olbrich, A.R., Ohlen, C., Greenberg, P. D., Stromnes, I.M., Iwashiro, M., Sakaguchi, S., Evans, L.H., Peterson, K.E., Yang, G., Hasenkrug, K.J., 2004. Functional impairment of CD8+ T cells by regulatory T cells during persistent retroviral infection. Immunity 20, 293–303.

Fleming, J.O., Trousdale, M.D., el-Zaatari, F.A., Stohlman, S.A., Weiner, L.P., 1986. Pathogenicity of antigenic variants of murine coronavirus JHM selected with monoclonal antibodies. J. Virol. 58, 869–875.

Fulton, R.B., Meyerholz, D.K., Varga, S.M., 2010. Foxp3+ CD4 regulatory T cells limit pulmonary immunopathology by modulating the CD8 T cell response during respiratory syncytial virus infection. J. Immunol. 185, 2382–2392.

Haeryfar, S.M., DiPaolo, R.J., Tscharke, D.C., Bennink, J.R., Yewdell, J.W., 2005. Regulatory T cells suppress CD8+ T cell responses induced by direct priming and cross-priming and moderate immunodominance disparities. J. Immunol. 174, 3344–3351.

Hindinger, C., Bergmann, C.C., Hinton, D.R., Phares, T.W., Parra, G.I., Hussain, S., Savarin, C., Atkinson, R.D., Stohlman, S.A., 2012. IFN-gamma signaling to astrocytes protects from autoimmune mediated neurological disability. PLoS One 7, e42088.

Ireland, D.D., Stohlman, S.A., Hinton, D.R., Atkinson, R., Bergmann, C.C., 2008. Type I interferons are essential in controlling neurotropic coronavirus infection irrespective of functional CD8 T cells. J. Virol. 82, 300–310.

Kapil, P., Atkinson, R., Ramakrishna, C., Cua, D.J., Bergmann, C.C., Stohlman, S.A., 2009. Interleukin-12 (IL-12), but not IL-23, deficiency ameliorates viral encephalitis without affecting viral control. J. Virol. 83, 5978–5986.

Korn, T., Reddy, J., Gao, W., Bettelli, E., Awasthi, A., Petersen, T.R., Backstrom, B.T., Sobel, R.A., Wucherpfennig, K.W., Strom, T.B., Oukka, M., Kuchroo, V.K., 2007. Myelin-specific regulatory T cells accumulate in the CNS but fail to control autoimmune inflammation. Nat. Med. 13, 423–431.

Langier, S., Sade, K., Kivity, S., 2010. Regulatory T cells: the suppressor arm of the immune system. Autoimmunity Rev. 10, 112–115.

Lee, D.C., Harker, J.A., Tregoning, J.S., Atabani, S.F., Johansson, C., Schwarze, J., Openshaw, P.J., 2010. CD25+ natural regulatory T cells are critical in limiting innate and adaptive immunity and resolving disease following respiratory syncytial virus infection. J. Virol. 84, 8790–8798.

Longhi, M.P., Wright, K., Lauder, S.N., Nowell, M.A., Jones, G.W., Godkin, A.J., Jones, S. A., Gallimore, A.M., 2008. Interleukin-6 is crucial for recall of influenza-specific memory CD4 T cells. PLoS Pathog. 4, e1000006.

Lourenco, E.V., La Cava, A., 2011. Natural regulatory T cells in autoimmunity. Autoimmunity 44, 33–42.

Lund, J.M., Hsing, L., Pham, T.T., Rudensky, A.Y., 2008. Coordination of early protective immunity to viral infection by regulatory T cells. Science 320, 1220–1224.

Madan, R., Demircik, F., Surianarayanan, S., Allen, J.L., Divanovic, S., Trompette, A., Yogev, N., Gu, Y., Khodoun, M., Hildeman, D., Boespflug, N., Fogolin, M.B., Grobe, L., Greweling, M., Finkelman, F.D., Cardin, R., Mohrs, M., Muller, W., Waisman, A., Roers, A., Karp, C.L., 2009. Nonredundant roles for B cell-derived IL-10 in immune counter-regulation. J. Immunol. 183, 2312–2320.

Marten, N.W., Stohlman, S.A., Bergmann, C.C., 2000. Role of viral persistence in retaining CD8+ T cells within the central nervous system. J. Virol. 74, 7903–7910.

Pewe, L., Perlman, S., 2002. Cutting edge: CD8 T cell-mediated demyelination is IFN-gamma dependent in mice infected with a neurotropic coronavirus. J. Immunol. 168, 1547–1551.

Phares, T.W., Stohlman, S.A., Hinton, D.R., Atkinson, R., Bergmann, C.C., 2010. Enhanced antiviral T cell function in the absence of B7-H1 is insufficient to prevent persistence but exacerbates axonal bystander damage during viral encephalomyelitis. J. Immunol. 185, 5607–5618.

Phares, T.W., Stohlman, S.A., Hwang, M., Min, B., Hinton, D.R., Bergmann, C.C., 2012. CD4 T cells promote CD8 T cell immunity at the priming and effector site during viral encephalitis. J. Virol. 86, 2416–2427.

Phares, T.W., Ramakrishna, C., Parra, G.I., Epstein, A., Chen, L., Atkinson, R., Stohlman, S.A., Bergmann, C.C., 2009. Target-dependent B7-H1 regulation contributes to clearance of central nervous system infection and dampens morbidity. J. Immunol. 182, 5430–5438.

Puntambekar, S.S., Bergmann, C.C., Savarin, C., Karp, C.L., Phares, T.W., Parra, G.I., Hinton, D.R., Stohlman, S.A., 2011. Shifting hierarchies of interleukin-10-producing T cell populations in the central nervous system during acute and persistent viral encephalomyelitis. J. Virol. 85, 6702–6713.

Richards, M.H., Getts, M.T., Podojil, J.R., Jin, Y.H., Kim, B.S., Miller, S.D., 2011. Virus expanded regulatory T cells control disease severity in the Theiler's virus mouse model of MS. J. Autoimmunity 36, 142–154.

Rouse, B.T., Sarangi, P.P., Suvas, S., 2006. Regulatory T cells in virus infections. Immunol. Rev. 212, 272–286.

Rowe, J.H., Ertelt, J.M., Way, S.S., 2012. Foxp3+ regulatory T cells, immune stimulation and host defence against infection. Immunology 136, 1–10.

Ruckwardt, T.J., Bonaparte, K.L., Nason, M.C., Graham, B.S., 2009. Regulatory T cells promote early influx of CD8+ T cells in the lungs of respiratory syncytial virus-infected mice and diminish immunodominance disparities. J. Virol. 83, 3019–3028.

Savarin, C., Bergmann, C.C., Hinton, D.R., Ransohoff, R.M., Stohlman, S.A., 2008. Memory CD4+ T-cell-mediated protection from lethal coronavirus encephalomyelitis. J. Virol. 82, 12432–12440.

Shalev, I., Wong, K.M., Foerste,r, K., Zhu, Y., Chan, C., Maknojia, A., Zhang, J., Ma, X.Z., Yang, X.C., Gao, J.F., Liu, H., Selzner, N., Clark, D.A., Adeyi, O., Phillips, M.J., Gorczynski, R.R., Grant, D., McGilvray, I., Levy, G., 2009. The novel CD4+CD25+ regulatory T cell effector molecule fibrinogen-like protein 2 contributes to the outcome of murine fulminant viral hepatitis. Hepatology 49, 387–397.

Sun, J., Dodd, H., Moser, E.K., Sharma, R., Braciale, T.J., 2011. CD4+ T cell help and innate-derived IL-27 induce Blimp-1-dependent IL-10 production by antiviral CTLs. Nat. Immunol. 12, 327–334.

Suvas, S., Azkur, A.K., Kim, B.S., Kumaraguru, U., Rouse, B.T., 2004. CD4+CD25+ regulatory T cells control the severity of viral immunoinflammatory lesions. J. Immunol. 172, 4123–4132.

Tang, Q., Adams, J.Y., Penaranda, C., Melli, K., Piaggio, E., Sgouroudis, E., Piccirillo, C.A., Salomon, B.L., Bluestone, J.A., 2008. Central role of defective interleukin-2 production in the triggering of islet autoimmune destruction. Immunity 28, 687–697.

Tirotta, E., Duncker, P., Oak, J., Klaus, S., Tsukamoto, M.R., Gov, L., Lane, T.E., 2013. Epstein-Barr virus-induced gene 3 negatively regulates neuroinflammation and T cell activation following coronavirus-induced encephalomyelitis. J. Neuroimmunol. 254, 110–116.

Trandem, K., Anghelina, D., Zhao, J., Perlman, S., 2010. Regulatory T cells inhibit T cell proliferation and decrease demyelination in mice chronically infected with a coronavirus. J. Immunol. 184, 4391–4400.

Trandem, K., Zhao, J., Fleming, E., Perlman, S., 2011a. Highly activated cytotoxic CD8 T cells express protective IL-10 at the peak of coronavirus-induced encephalitis. J. Immunol. 186, 3642–3652.

Trandem, K., Jin, Q., Weiss, K.A., James, B.R., Zhao, J., Perlman, S., 2011b. Virally expressed interleukin-10 ameliorates acute encephalomyelitis and chronic demyelination in coronavirus-infected mice. J. Virol. 85, 6822–6831.

Weiss, J.M., Bilate, A.M., Gobert, M., Ding, Y., Curotto de Lafaille, M.A., Parkhurst, C. N., Xiong, H., Dolpady, J., Frey, A.B., Ruocco, M.G., Yang, Y., Floess, S., Huehn, J., Oh, S., Li, M.O., Niec, R.E., Rudensky, A.Y., Dustin, M.L., Littman, D.R., Lafaille, J.J., 2012. Neuropilin 1 is expressed on thymus-derived natural regulatory T cells, but not mucosa-generated induced Foxp3+ T reg cells. J. Exp. Med. 209, 1723–1742.

Weiss, S.R., Leibowitz, J.L., 2011. Coronavirus pathogenesis. Adv. Virus Res. 81, 85–164.

Wojno, E.D., Hunter, C.A., 2012. New directions in the basic and translational biology of interleukin-27. Trends Immunol. 33, 91–97.

Xu, D., Fu, J., Jin, L., Zhang, H., Zhou, C., Zou, Z., Zhao, J.M., Zhang, B., Shi, M., Ding, X., Tang, Z., Fu, Y.X., Wang, F.S., 2006. Circulating and liver resident CD4+CD25+ regulatory T cells actively influence the antiviral immune response and disease progression in patients with hepatitis B. J. Immunol. 177, 739–747.

Yadav, M., Louvet, C., Davini, D., Gardner, J.M., Martinez-Llordella, M., Bailey-Bucktrout, S., Anthony, B.A., Sverdrup, F.M., Head, R., Kuster, D.J., Ruminski, P., Weiss, D., Von Schack, D., Bluestone, J.A., 2012. Neuropilin-1 distinguishes natural and inducible regulatory T cells among regulatory T cell subsets in vivo. J. Exp. Med. 209, 1713–1722.

Zelinskyy, G., Dietze, K.K., Husecken, Y.P., Schimmer, S., Nair, S., Werner, T., Gibbert, K., Kershaw, O., Gruber, A.D., Sparwasser, T., Dittmer, U., 2009. The regulatory T-cell response during acute retroviral infection is locally defined and controls the magnitude and duration of the virus-specific cytotoxic T-cell response. Blood 114, 3199–3207.

Zhao, J., Zhao, J., Perlman, S., 2012. Differential effects of IL-12 on Tregs and non-Treg T cells: roles of IFN-gamma, IL-2 and IL-2R. PLoS One 7, e46241.

Zhao, J., Fett, C., Trandem, K., Fleming, E., Perlman, S., 2011. IFN-gamma- and IL-10-expressing virus epitope-specific Foxp3+ T reg cells in the central nervous system during encephalomyelitis. J. Exp. Med. 208, 1571–1577.